

# Estrogen Regulates Adrenal Angiotensin AT<sub>1</sub> Receptors by Modulating AT<sub>1</sub> Receptor Translation

ZHENG WU, CHRISTINE MARIC, DARREN M. ROESCH, WEI ZHENG, JOSEPH G. VERBALIS, AND KATHRYN SANDBERG

*Departments of Physiology and Biophysics (Z.W., K.S.) and Medicine (C.M., D.M.R., W.Z., J.G.V., K.S.), Georgetown University, Washington, D.C. 20007*

**Hypertension and associated cardiovascular disease increase after menopause. Angiotensin AT<sub>1</sub> receptor (AT<sub>1</sub>R) antagonists are effective treatments, in part, by inhibiting angiotensin II (Ang II)-induced aldosterone release from the adrenal zona glomerulosa (ZG). Estrogen decreases the number of AT<sub>1</sub>Rs in the adrenal gland and attenuates acute Ang II-induced aldosterone release. Here, we examined the effects of 17 $\beta$ -estradiol (E<sub>2</sub>) on AT<sub>1</sub>R gene regulation in the rat adrenal cortex (AC). Female rats were ovariectomized and injected with vehicle or E<sub>2</sub>. Immunohistochemistry revealed the presence of both estrogen receptor (ER) $\alpha$  and ER $\beta$  in the ZG, and E<sub>2</sub> treatment increased the intensity of their nuclear staining. Under conditions in which AT<sub>1</sub>R maximal binding capacity was decreased by 46%, chronic miniosmotic pump Ang II-induced aldosterone secretion was reduced by 43%. E<sub>2</sub> treat-**

**ment had no effect on AT<sub>1a</sub>R and AT<sub>1b</sub>R mRNA levels in the AC, whereas the AT<sub>1</sub>R mRNA polysome distribution in sucrose gradients was shifted to lighter fractions, indicating that E<sub>2</sub> treatment reduces AT<sub>1</sub>R translation. RNA binding proteins (RBPs) in AC extracts formed complexes with the 5' leader sequence (5'LS), coding region, and the 3'-untranslated region (3'UTR); however, only the activity of 5'LS RBPs was regulated by E<sub>2</sub> treatment. These data suggest that E<sub>2</sub>, acting through its receptors in the ZG, reduces AT<sub>1</sub>R density and Ang II-induced aldosterone release, primarily by inhibiting AT<sub>1</sub>R translation, possibly by blocking ribosomal scanning caused by increased steric hindrance from 5'LS RBPs. Dysregulation of this posttranscriptional mechanism may contribute to the increased incidence of cardiovascular disease associated with menopause. (*Endocrinology* 144: 3251–3261, 2003)**

**I**N WOMEN, THE incidence of cardiovascular disease dramatically increases after menopause (1). Although the recent findings from the Women's Health Initiative trial have questioned the role of combined estrogen-progestin hormone replacement therapy in protecting postmenopausal women against cardiovascular disease (2, 3), numerous studies indicate that estrogen deficiency in postmenopausal women increases the risk of developing hypertension, coronary atherosclerosis, and myocardial infarction (4–6). Furthermore, many studies suggest that estrogen therapy has cardiovascular protective benefits by lowering blood pressure, increasing cardiac output, and reducing the risk of developing coronary atherosclerosis and myocardial infarction (7–9).

Estrogen is associated with a lipid profile in women that includes reduced low-density and elevated high-density lipoprotein levels. This cardioprotective lipid profile contrasts with the atherogenic lipid profile that often develops after menopause. Estrogen is also associated with improved endothelial function. By elevating nitric oxide and prostaglandin levels, estrogen enhances vasodilation, inhibits proliferation of vascular smooth muscle cells, and reduces platelet

aggregation and is thereby thought to attenuate atherosclerosis (10). Nonetheless, analyses of large-scale studies indicate that the benefits of estrogen on the lipid profile account for only 25–50% of the cardioprotective effects associated with the hormone, suggesting that additional factors are involved (11).

In addition to estrogen deficiency, another recognized factor implicated in the pathogenesis of hypertension, atherosclerosis, and congestive heart failure is overactivation of the renin-angiotensin system (RAS). Inhibition of the RAS by angiotensin-converting enzyme inhibitors and angiotensin AT<sub>1</sub> receptor (AT<sub>1</sub>R) antagonists are effective treatment modalities for these disease states (12). Accumulating data indicates that estrogen regulates all of the known components of the RAS. The synthesis of angiotensinogen in hepatocytes is regulated by estrogen (13). Plasma renin levels and angiotensin-converting enzyme activity are significantly higher in estrogen-deficient (compared with estrogen-replete) rats and in postmenopausal women not receiving ERT (compared with women who do) (5, 6). Concordantly, circulating levels of angiotensin II (Ang II) are higher in estrogen-deficient monkeys and transgenic hypertensive rats, compared with their estrogen-replete counterparts (14, 15). We and others have shown that, in addition to regulating the components involved in synthesizing Ang II, estrogen also alters the expression of AT<sub>1</sub>Rs in many target tissues (16–18). Estrogen attenuates vascular responses to Ang II (19), and we have recently observed that, in the presence of peak physiological levels of estrogen, when adrenal AT<sub>1</sub>R expression is reduced by approximately 30% (18), adrenal responsiveness to acute Ang II surges is markedly attenuated (20); Ang

Abbreviations: AC, Adrenal cortex; Ang II, angiotensin II; AT<sub>1</sub>R, angiotensin AT<sub>1</sub> receptor; Bmax, maximal binding capacity; CR, coding region; DAB, 3,3'-diaminobenzidine tetrachloride dihydrate; E<sub>2</sub>, 17 $\beta$ -estradiol; ER, estrogen receptor; 5'LS, 5' leader sequence; ERE, estrogen response elements; FL, full-length; ns, not significant; nt, nucleotide(s); OAT, ornithine  $\delta$ -aminotransferase; OVX, ovariectomized; RAS, renin-angiotensin system; RBP, RNA binding protein; RNase, ribonuclease; RPA, ribonuclease protection assay; UTR, untranslated region; ZF, zona fasciculata; ZG, zona glomerulosa; ZR, zona reticularis.

II-induced aldosterone production was reduced by 45% in 17 $\beta$ -estradiol (E<sub>2</sub>)-treated ovariectomized (OVX) rats fed a NaCl-deficient diet, compared with estrogen-deficient animals.

Aldosterone serves as an important mediator of fluid homeostasis and blood pressure control, and recent studies indicate that rapid increases in circulating aldosterone can modify sympathetic outflow to the heart, vasculature, and kidney through effects in the brain (21). Rats treated chronically with mineralocorticoids develop hypertension (22). Accompanying features of mineralocorticoid-induced hypertension include several risk factors for cardiovascular events, such as increased vascular responsiveness to Ang II, increased vascular resistance, and decreased baroreflex sensitivity. Furthermore, inhibition of aldosterone receptors with spironolactone was recently shown, in the Randomized Aldactone Evaluation Study, to substantially reduce the risk of morbidity and mortality among patients with severe heart failure who were also receiving standard angiotensin-converting enzyme inhibition therapy (23). Thus, estrogen-induced decreases in acute levels of Ang II-induced aldosterone secretion may contribute to the cardiovascular benefits associated with estrogen by decreasing overall mineralocorticoid activity; and conversely, a loss in the ability to down-regulate AT<sub>1</sub>Rs and Ang II-induced aldosterone release in estrogen-deficient states may represent a risk factor for hypertension and cardiovascular events associated with aging and menopause. In this study, we investigated the molecular mechanisms underlying E<sub>2</sub> regulation of AT<sub>1</sub>R gene expression in the rat adrenal gland.

## Materials and Methods

### Animal treatment

Female Sprague Dawley rats, weighing approximately 250–300 g, were obtained from Harlan Inc. (Indianapolis, IN). All rats were subjected to ovariectomy; and the following day, they were treated with either a daily injection of vehicle (peanut oil) or vehicle containing E<sub>2</sub>. In the time course study, animals were treated with 40  $\mu$ g/kg E<sub>2</sub> for 2, 4, 8, and 16 d. In the dose response study, OVX rats were injected with E<sub>2</sub> at 10, 25, 40, and 50  $\mu$ g/kg for 8 d. For all other studies, rats were injected with vehicle or E<sub>2</sub> at 40  $\mu$ g/kg every day for 8 d. All rats were maintained on a phytoestrogen-free diet (TD95092, Harlan Inc.) and tap water *ad libitum*. After experimental treatments, rats were killed by decapitation, and tissues were rapidly excised, snap-frozen in liquid nitrogen, and stored at –80 C. For immunohistochemistry, the adrenal glands were removed and fixed with 4% paraformaldehyde for 3 h at room temperature.

### Measurement of plasma E<sub>2</sub> levels

Blood (0.5–1 ml) was collected, and the plasma was separated by centrifugation. E<sub>2</sub> levels were measured according to the RIA protocol of Diagnostic Products (Los Angeles, CA).

### Immunohistochemistry of estrogen receptors (ERs)

After fixation, the adrenal gland was routinely processed to paraffin; 4- $\mu$ m sections were cut and placed on 1% gelatinized slides. Sections were incubated with 10% nonimmune goat serum for 30 min at room temperature, then with the ER $\alpha$  (MC-20, rabbit polyclonal IgG; Santa Cruz Biotechnology, Inc., Santa Cruz, CA) or the ER $\beta$  (PAI-313, rabbit polyclonal IgG; Affinity BioReagents, Inc., Golden, CO) antisera at 4 C overnight. The endogenous peroxidase was removed by incubation with 1% H<sub>2</sub>O<sub>2</sub> for 10 min. After washes with PBS (3  $\times$  5 min), the sections were incubated with biotinylated goat-antirabbit IgG (DAKO Corp.,

Copenhagen, Denmark) for 1 h at room temperature, followed by a 10-min treatment with 3,3'-diaminobenzidine tetrachloride dihydrate (DAB) containing 3% H<sub>2</sub>O<sub>2</sub>. Sections were counterstained with Mayer's hematoxylin to allow anatomical definition of adrenal layers. A positive reaction was identified as a brown stain in the cytoplasm, or a black nuclear stain as a result of superimposition of the DAB reaction and the blue counterstain. Sections incubated with 10% nonimmune goat serum, instead of the primary antiserum, were used as negative controls. Sections were imaged by light microscopy.

### Radioligand binding assay

The adrenal cortex (AC) was separated from the medulla, yielding a sample of AC that mainly contained the zona glomerulosa (ZG) and outer portions of the zona fasciculata (ZF). Cell membranes from whole homogenized adrenal glands or the AC were prepared and used in radioligand binding assays as previously described (18). <sup>125</sup>I-[Sar<sup>1</sup>, Ile<sup>8</sup>]Ang II (0.05–4.0 nM) was incubated with adrenal gland (15  $\mu$ g) or AC (5  $\mu$ g) membranes at room temperature for 3 h in binding buffer (100 mM NaCl; 10 mM Na<sub>2</sub>HPO<sub>4</sub>; 5 mM EDTA, pH 7.4) supplemented with 0.1% BSA in the presence of 5  $\mu$ M of the type 2 angiotensin receptor antagonist, PD-123,319 (to determine only AT<sub>1</sub>R densities). Nonspecific binding was determined in the presence of unlabeled Ang II at 250 nM (based on the fact that this concentration is 100 times the dissociation constant for Ang II at the AT<sub>1</sub>R). AT<sub>1</sub>R densities [maximal binding capacity (B<sub>max</sub>)] were determined by Scatchard analysis using a computerized nonlinear regression analysis of the saturation isotherm data software program, PRISM (GraphPad Software, Inc., San Diego, CA).

### Measurement of chronic Ang II-induced aldosterone secretion

OVX rats were implanted with miniosmotic pumps (Alzet model 2001; Durect Corporation, Cupertino, CA) delivering vehicle (sterile 0.9% NaCl, n = 23) or Ang II at a rate of 200 ng/kg-min (n = 24). Half the animals in each group were treated with vehicle (peanut oil), and half were treated with E<sub>2</sub> at 40  $\mu$ g/kg for 8 d. The resulting experimental groups were: OVX (n = 11), E<sub>2</sub>-treated (n = 12), Ang II-infused (n = 12), and the combination E<sub>2</sub> treatment and Ang II-infusion (n = 12). On the 8th day, the rats were anesthetized with isoflurane (3% in O<sub>2</sub> flowing 0.5 liters/min), and heparinized blood was collected via cardiac puncture. The rats were immediately killed by decapitation. Plasma aldosterone concentrations were determined according to the RIA protocol of Diagnostic Products.

### Preparation of radiolabeled RNA

The 5' leader sequence (5'LS) and coding region (CR) of the rat AT<sub>1a</sub>R and AT<sub>1b</sub>R cDNAs were subcloned into the pCR3 vector by TA cloning (Invitrogen, Carlsbad, CA). The full-length (FL) rat AT<sub>1a</sub>R and AT<sub>1b</sub>R cDNAs were subcloned into the pcDNA1/Amp vector (Invitrogen) (24). Three regions of the CR (CR-1, 133–348; CR-2, 532–764; CR-3, 776–991) and 3 regions of the 3' untranslated region (UTR) (3'UTR-1, 1396–1609; 3'UTR-2, 1590–1812; 3'UTR-3, 1954–2157) were randomly selected from the AT<sub>1a</sub>R cDNA and subcloned into pGEM-Teasy vector by TA cloning (Invitrogen).

To prepare <sup>32</sup>P-labeled antisense RNA probes for the ribonuclease (RNase) protection assay (RPA), the CR-AT<sub>1a</sub>R cDNA in pCR3 was linearized with Acc I to generate CR-4. The 3'UTR RNA probes were prepared from FL-AT<sub>1a</sub>R and FL-AT<sub>1b</sub>R cDNAs in the pcDNA1/Amp plasmid by linearizing with Bsa B1 and Psh A1, to generate 3'UTR-4 and 3'UTR-5, respectively. Linearized pTRI- $\beta$ -actin plasmid was purchased from Ambion, Inc. (Austin, TX) (RPAlII kit). To prepare <sup>32</sup>P-labeled RNA sense probes for the RNA EMSA, the AT<sub>1a</sub>- and AT<sub>1b</sub>-5'LS pCR3 plasmids were linearized by Xho I. The CR-1, CR-2, CR-3, 3'UTR-1, 3'UTR-2, and 3'UTR-3 in pGEM-Teasy plasmids were linearized by Sac II or Not I.

Linearized DNA templates (1  $\mu$ g) were incubated with T7 or SP6 RNA polymerase and 50  $\mu$ Ci [ $\alpha$ -<sup>32</sup>P]GTP or [ $\alpha$ -<sup>32</sup>P]CTP, according to the protocol of Promega Corp. (Madison, WI) for *in vitro* synthesis of high-specific-activity single-stranded RNA probes. Radiolabeled RNA probes were purified on 8 M urea-5% polyacrylamide gels. Once eluted from the gels, RNA probes were precipitated with 7.5 M ammonium acetate, pH 6.0, and 100% ethanol (at a ratio of 0.1–3 X, respectively, where X is

the gel elution volume) and resuspended in diethyl pyrocarbonate-treated H<sub>2</sub>O.

### RPA

RNA from AC and pituitary was isolated by TRIZOL reagent (Invitrogen), and RNA concentrations were determined by the Ribogreen RNA quantitation method (Molecular Probes, Inc., Eugene, OR). Total RNA (20–30 µg) was incubated with approximately 30,000–40,000 cpm of 3'UTR-4 (AT<sub>1a</sub>R) or 3'UTR-5 (AT<sub>1b</sub>R) <sup>32</sup>P-labeled antisense probes, according to Ambion, Inc.'s RPA III protocol. RNA isolated from the sucrose gradient fractions was incubated with CR-4 (AT<sub>1a</sub>R and AT<sub>1b</sub>R) <sup>32</sup>P-labeled antisense probe. The sizes of the 3'UTR-4, 3'UTR-5 or CR-4 radiolabeled probes were 462 nucleotides (nt), 469 nt, and 139 nt, whereas the protected sizes were 420 nt, 429 nt, and 89 nt, respectively (note, the protected fragments were slightly smaller than radiolabeled probes before treatment with T1 RNase because 40 nt of RNA encoded by the plasmid used to generate the probes was included in the probe; consequently, this plasmid RNA was degraded by T1RNase). A total of 25,000 cpm mouse pTRI-β-actin antisense probe (full probe size = 304 nt; protected size = 250 nt) was added to the incubations to control for RNA integrity and gel loading. In negative controls, 2.5 µg yeast RNA was hybridized with the antisense probes, followed by incubation with and without T1 RNase.

Samples were loaded onto 8 M urea-5% polyacrylamide gels and electrophoresed at 200 V for 90 min. Dried gels were exposed to a phosphorimager screen (Molecular Dynamics, Inc., Piscataway, NJ), and the abundance of AT<sub>1</sub>R mRNA was quantitated by ImageQuant software (IQMac version 1.2; Molecular Dynamics, Inc.). We chose to analyze the autoradiograms by phosphorimaging over optical density measured by scanning densitometry, because phosphorimaging is more sensitive, and the magnitude of the linear range significantly greater, than optical density. Initially, we performed an RNA dose-response curve in the RPA. The doses we chose (AC, 30 µg; pituitary, 35 µg) were well within the linear range of the phosphorimaging analysis, even for the light AT<sub>1a</sub>R bands detected in the pituitary.

### Polysomal distribution analysis

Polysome analysis was essentially carried out as previously described (25) and is based on the principle that the largest polysomes (multiple ribosomes bound to a single mRNA) are denser and, therefore, will sediment faster through a sucrose gradient than monosomes (one ribosome bound to a mRNA) or free ribosomal subunits not bound to mRNA (26). In brief, extracts from AC were homogenized in 3 ml ice-cold buffer A (20 mM Tris HCl, pH 7.5; 100 mM NaCl; 1.5 mM MgCl<sub>2</sub>) supplemented with 10 mM EGTA, 500 µg/ml heparin, 0.5% Triton X-100, 100 µg/ml cycloheximide, 0.5% deoxycholic acid, and 160 U/ml RNasin inhibitor. After centrifugation at 12,000 × g for 10 min at 4 C, the supernatants were loaded onto 10–50% linear sucrose gradients prepared in buffer A. In the polysome disruption experiment, the supernatant was loaded onto a sucrose gradient prepared in buffer A devoid of MgCl<sub>2</sub> and supplemented with 20 mM EDTA. The gradient was centrifuged at 243,000 × g in a SW40Ti rotor (Beckman, Fullerton, CA) at 4 C for 2 h. Six equal volume fractions were collected from the bottom to the top of the sucrose gradient, and equal volumes of buffer B (0.2 M Tris HCl, pH 7.5; 25 mM EDTA; 0.3 M NaCl; and 0.2% sodium dodecyl sulfate) were added to the sucrose fractions. After digestion with 500 µg/ml pronase (Sigma, St. Louis, MO) at 37 C for 30 min, RNA was extracted by phenol-chloroform and precipitated with 3 M sodium acetate (pH 5.2) and ethanol. The RNA pellet was dissolved in diethyl pyrocarbonate-treated H<sub>2</sub>O.

The amount of AT<sub>1</sub>R mRNA in each fraction was determined by RPA using the CR-4 radiolabeled antisense RNA probe (note, this probe detects both AT<sub>1a</sub>R and AT<sub>1b</sub>R mRNA levels attributable to the high nucleotide sequence homology in this region). Sample variation in cytoplasmic levels of AT<sub>1</sub>R mRNA was controlled by normalizing the AT<sub>1</sub>R mRNA recovered in each fraction, to the total amount of AT<sub>1</sub>R mRNA recovered from the entire fractionation. Animal-to-animal variation was minimized, because each n value constituted a sucrose fractionation from the adrenals of six animals. Variation between fractionations was evaluated statistically by calculating the SE of the mean from multiple fractionations. At least three fractionations were performed for

each experimental group. Sucrose gradient and RPA assays for each experimental group were run in parallel.

### Preparation of cytosolic extract

Extracts from the AC were homogenized in a buffer containing 25 mM Tris HCl, pH 7.4; 0.1 mM EDTA; 1% Triton X-100; 40 mM KCl and supplemented with protease inhibitors, as previously described (18). Samples were layered on top of a 30% sucrose cushion and centrifuged at 230,000 × g for 3 h at 4 C. The supernatant (referred to as cytosolic extract) was collected and stored at –80 C. The protein concentration of the cytosolic extract was measured, using a colorimetric assay (Bio-Rad Laboratories, Inc., Hercules, CA), using BSA as a standard.

### RNA EMSA

Cytosolic extracts from AC were incubated with 100,000 cpm <sup>32</sup>P-labeled 5'LS(AT<sub>1a</sub>R), 5'LS(AT<sub>1b</sub>R), CR-1, CR-2, CR-3, 3'UTR-1, 3'UTR-2, 3'UTR-3 RNA probes, as described previously (18). After T1 RNase treatment and heparin digestion, samples were electrophoresed at 200 V for 3 h in a 4% polyacrylamide gel. Dried gels were exposed to a phosphorimager screen (Molecular Dynamics, Inc.), and RNA binding protein (RBP) activity was quantitated by ImageQuant software (IQMac version 1.2; Molecular Dynamics, Inc.).

### Statistical analysis

The value of each group was averaged, and the SEM was calculated. Results are expressed as the mean ± SEM. Statistical analyses were performed by one-way ANOVA, followed by Newman-Keuls test for multiple group comparison. Comparisons between two groups were made by unpaired *t* test. *P* values less than 0.05 were considered statistically significant, whereas values of at least 0.05 or greater were considered not significant (ns).

## Results

### *E*<sub>2</sub> increases the intensity of ERα and ERβ nuclear immunolocalization

To determine the effect of E<sub>2</sub> on ER subtype protein expression and location within the adrenal gland, we used an immunohistochemical approach. In OVX rats, ERα subtype immunoreactivity was found in many cells throughout the AC, including the ZG, ZF, and zona reticularis (ZR) (Fig. 1A), and in a few isolated cells of the adrenal medulla (not shown), whereas the ERβ subtype was confined mainly to the ZG (Fig. 1C). In contrast to the ERα staining that was found mostly in the cytoplasm, ERβ staining was observed more in cell nuclei. E<sub>2</sub> treatment markedly increased the number of cells with nuclear staining of ERα in the ZG and ZF (Fig. 1B), and revealed ERβ-positive nuclei in the ZF and ZR that were not observed in the estrogen-deficient OVX animals (Fig. 1D). No immunoreactivity was observed in any sections incubated with nonimmune serum instead of the primary antibody for ERα or ERβ, as evidenced by the presence of only blue counterstained stained cell nuclei in OVX (Fig. 1E) and OVX + E<sub>2</sub> (Fig. 1F) animals. No significant changes in either the intensity or the pattern of ERα or ERβ staining were seen in the adrenal medulla with E<sub>2</sub> treatment (not shown).

### *E*<sub>2</sub> reduces adrenal AT<sub>1</sub>R density in a time- and dose-dependent manner

To determine the time course and dose response of E<sub>2</sub> regulation of AT<sub>1</sub>R density, saturation isotherms using [<sup>125</sup>I]-[Sar<sup>1</sup>, Ile<sup>8</sup>]Ang II (Fig. 2A) were performed on AC mem-

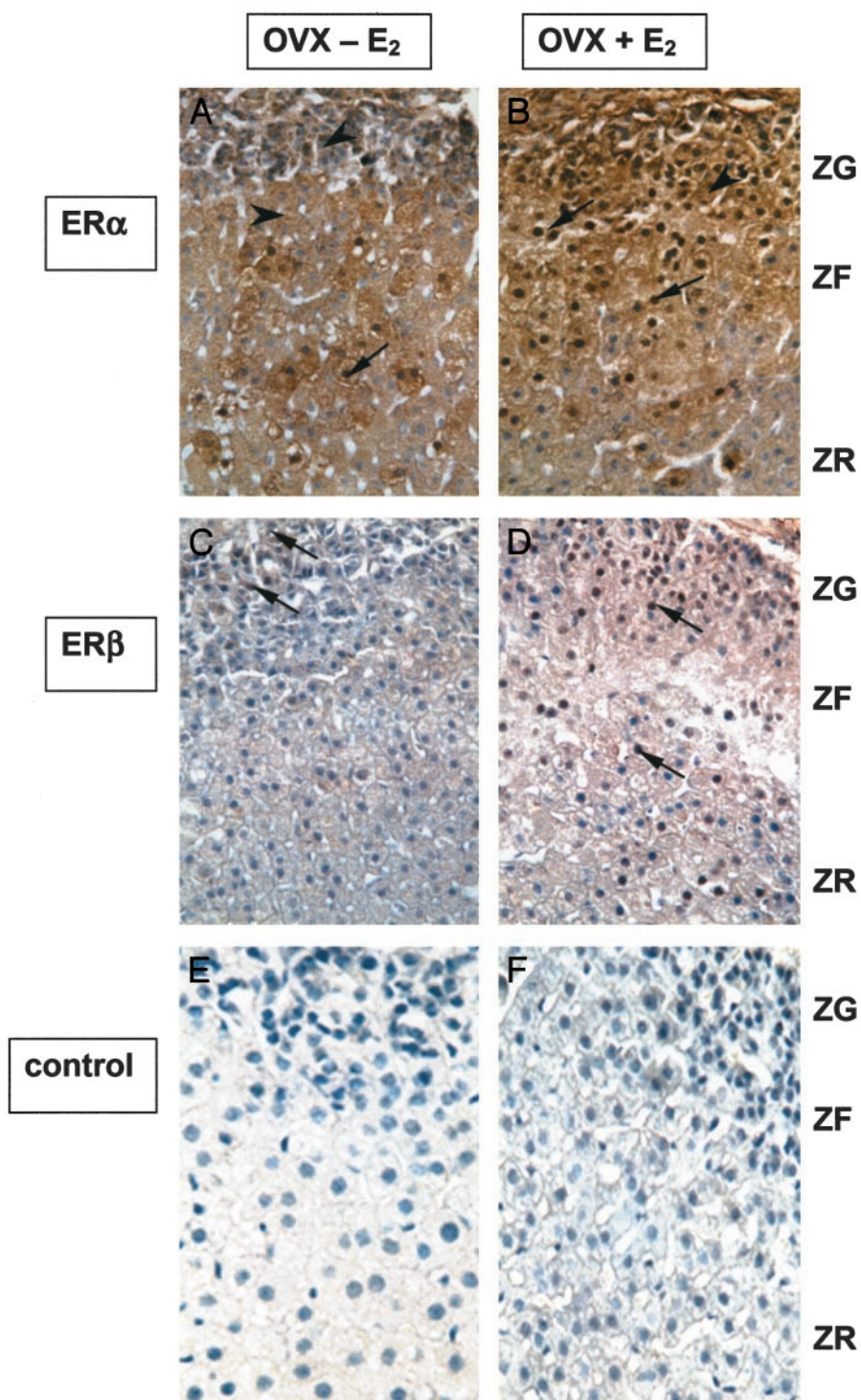


FIG. 1. Effect of E<sub>2</sub> treatment on localization of ER $\alpha$  and ER $\beta$  in the AC. All sections were counterstained with Meyers hematoxylin, so a positive reaction was identified as a brown stain in the cytoplasm, or a brown-black nuclear stain as a result of superimposition of the DAB reaction product and the blue counterstain. ER $\alpha$  immunoreactivity of vehicle-treated OVX animals (A) was observed in the cytoplasm of numerous cells of the ZG, ZF, and ZR (arrowheads), and, in a smaller number of cells, as nuclear staining (arrows). ER $\alpha$  immunoreactivity in the OVX+E<sub>2</sub> animals (B) was also observed in the cytoplasm (arrowheads) but was seen in the nucleus of a larger number of cells in all layers of the cortex (arrows). ER $\beta$  immunoreactivity of vehicle-treated OVX animals (C) was observed primarily in nuclei in the cells of the ZG (arrows). ER $\beta$  immunoreactivity in OVX+E<sub>2</sub> animals (D) was observed in the nuclei of a greater number of cells in the ZG and ZF (arrows). No immunoreactivity was observed in sections from OVX (E) and OVX + E<sub>2</sub> (F) rats that were incubated with nonimmune serum. Magnification, approximately  $\times 400$ .

branes prepared from OVX rats injected with E<sub>2</sub> for 2, 4, 8, and 16 d (Fig. 2B). E<sub>2</sub> significantly decreased AT<sub>1</sub>R Bmax, by 15%, after 2 d of treatment; maximum reductions in AT<sub>1</sub>R number were obtained after 8 d (Fig. 2B). A dose-response study, after 8 d, showed that E<sub>2</sub> treatment reduced AT<sub>1</sub>R Bmax in a gradual dose-dependent manner; significant reductions (18%) in AT<sub>1</sub>R Bmax were observed at 10  $\mu\text{g}/\text{kg}$ , and even greater reductions (41%) were observed at the peak dose of E<sub>2</sub> studied (50  $\mu\text{g}/\text{kg}$ ) (Fig. 2C).

Based on the time course and dose response, we carried out all further experiments in OVX rats treated with 40  $\mu\text{g}/\text{kg}$  E<sub>2</sub> for 8 d, because these conditions caused a marked 30% decrease in adrenal AT<sub>1</sub>R number without significantly altering receptor binding affinities (dissociation constant, pM: OVX,  $100 \pm 7$ ; OVX + E<sub>2</sub>,  $88 \pm 6$ , ns vs. OVX) (Fig. 2A). Radioligand binding on membranes prepared from AC homogenates showed that E<sub>2</sub> treatment similarly decreased AT<sub>1</sub>R Bmax by 46% (fmol/mg: OVX,

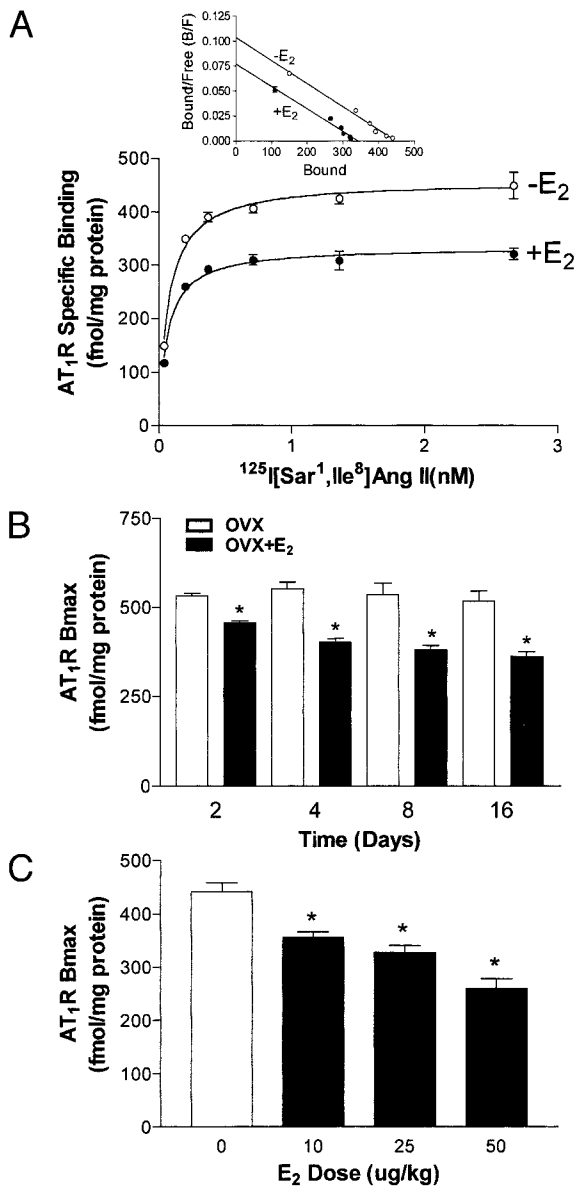


FIG. 2. Effect of E<sub>2</sub> treatment on adrenal AT<sub>1</sub>R expression. Adrenal membranes were incubated with increasing concentrations of [<sup>125</sup>I]-[Sar<sup>1</sup>, Ile<sup>8</sup>]Ang II in the presence of saturating concentrations of the type 2 angiotensin receptor blocker, PD-123,319 (so only AT<sub>1</sub>Rs were measured) in the absence (for determination of total receptor binding) or presence of 250 nM Ang II (for determination of nonspecific binding). A, Saturation isotherms. Shown are saturation isotherms of [<sup>125</sup>I]-[Sar<sup>1</sup>, Ile<sup>8</sup>]Ang II binding to adrenal membranes prepared from OVX rats treated with vehicle (peanut oil) (open circles) or E<sub>2</sub> at 40 μg/kg·d (filled circles) for 8 d. The data are averaged from three experiments, each performed in duplicate (each n value constitutes two animals/group; n = 3). Inset, Scatchard plot, derived from saturation binding data using the software program, PRISM. B, Time course. Shown are the Bmax values from OVX rats treated with vehicle (open bars) or E<sub>2</sub> at 40 μg/kg·d (filled bars) for 2, 4, 8, or 16 d. The values were derived by computerized nonlinear regression analysis of the saturation isotherm data (as in A), using the program, PRISM. \*, P < 0.001, OVX vs. OVX + E<sub>2</sub>; n = 6. C, Dose response. Shown are the Bmax values from OVX rats treated with vehicle (open bar) and E<sub>2</sub> (filled bars) at doses of 10, 25, or 50 μg/kg·d. The values were derived by a computerized nonlinear regression analysis of the saturation isotherm data (as in A), using the program, PRISM. \*, P < 0.01, OVX vs. OVX + E<sub>2</sub>, n = 3.

311 ± 18; OVX + E<sub>2</sub>, 168 ± 14, P < 0.05 vs. OVX, n = 4). Under these conditions, plasma E<sub>2</sub> levels in vehicle-treated rats were only 3.4 ± 0.5 pg/ml (n = 10), which is the level typically detected at estrus, whereas plasma E<sub>2</sub> levels in E<sub>2</sub>-treated OVX rats were 120 ± 10 pg/ml (n = 11), which represents the peak physiological level reached during the estrous cycle (27).

#### E<sub>2</sub> attenuates chronic Ang II-induced aldosterone secretion

To determine the effect of E<sub>2</sub> on chronic aldosterone secretion, we measured plasma aldosterone levels in OVX ± E<sub>2</sub>-treated rats after chronic infusion of Ang II via miniosmotic pumps (Fig. 3). E<sub>2</sub> treatment did not significantly alter basal plasma aldosterone levels (pg/ml: OVX, 150 ± 34, n = 11; OVX + E<sub>2</sub>, 250 ± 56, n = 12, ns vs. OVX). In contrast, chronic Ang II infusion in OVX rats significantly increased plasma aldosterone concentration (by 221%, to 482 ± 64 pg/ml, n = 12, P < 0.05 vs. OVX). E<sub>2</sub> treatment significantly reduced Ang II-induced aldosterone secretion (by 43%, to 276 ± 93 pg/ml, n = 12, P < 0.05 vs. Ang II-infused OVX).

#### E<sub>2</sub> does not alter AT<sub>1a</sub>R and AT<sub>1b</sub>R mRNA levels in the AC

To distinguish between AT<sub>1a</sub>R and AT<sub>1b</sub>R mRNA expression, we developed an RPA that distinguished between AT<sub>1a</sub>R and AT<sub>1b</sub>R mRNA expression by designing AT<sub>1</sub>R subtype-specific <sup>32</sup>P-labeled 3'UTR antisense probes (3'UTR-4 and 3'UTR-5, respectively). No cross-reactivity between AT<sub>1a</sub>R and AT<sub>1b</sub>R mRNA antisense probes was observed under the conditions of the RPA (data not shown). β-actin mRNA levels were also measured using a <sup>32</sup>P-β-actin probe, to control for RNA integrity and gel loading. The steady-state mRNA levels of AT<sub>1a</sub>R and AT<sub>1b</sub>R were expressed as the ratio of AT<sub>1a</sub>R or AT<sub>1b</sub>R mRNA to β-actin mRNA.

Both AT<sub>1</sub>R subtypes were enriched in the AC (Fig. 4, A and B). The results also demonstrate that, under conditions in which E<sub>2</sub> markedly decreased AT<sub>1</sub>R density, E<sub>2</sub> had no significant effects on either AT<sub>1a</sub>R or AT<sub>1b</sub>R mRNA levels in the

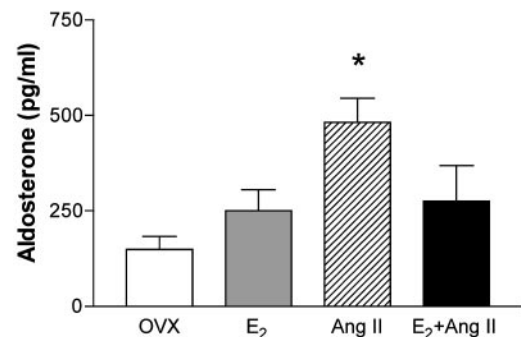


FIG. 3. Effect of E<sub>2</sub> treatment on chronic Ang II-induced aldosterone secretion. OVX rats were implanted with miniosmotic pumps delivering vehicle (sterile 0.9% NaCl) or Ang II at 200 ng/kg·min for the duration of the experiment. Half the rats in each group were treated with vehicle or E<sub>2</sub> at 40 μg/kg·d for 8 d (conditions that are identical to those shown in Fig. 2A). Plasma aldosterone was determined by RIA in the following experimental groups: OVX (n = 11) (open bar), Ang II-infused (n = 12) (gray bar), E<sub>2</sub>-treated (n = 12) (striped bar), and combined E<sub>2</sub> treatment and Ang II-infusion (n = 12) (black bar). \*, P < 0.05 vs. OVX, E<sub>2</sub>, and E<sub>2</sub> + Ang II.

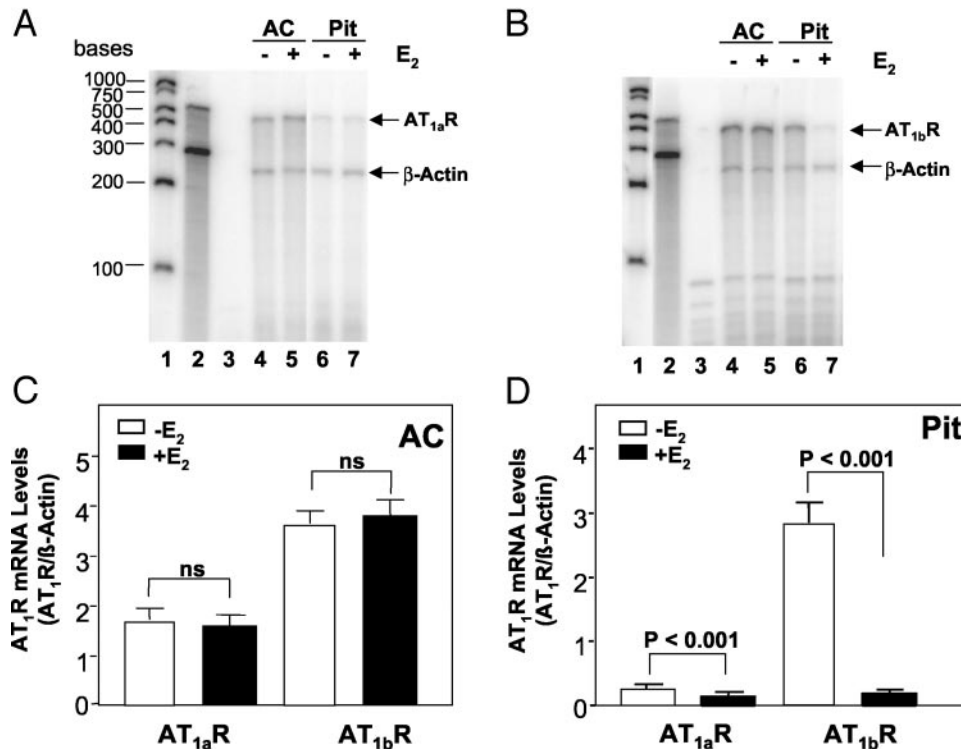


FIG. 4. Effect of E<sub>2</sub> treatment on AT<sub>1a</sub>R and AT<sub>1b</sub>R mRNA levels in the adrenal and pituitary. Total RNA isolated from AC (30 μg) (A and B, lanes 4 and 5) or pituitary (Pit) (35 μg) (A and B, lanes 6 and 7) from OVX rats treated with vehicle (lanes 4 and 6) or E<sub>2</sub> (lanes 5 and 7) (conditions identical to those shown in Fig. 2A) was incubated with 25,000 cpm β-actin and 35,000 cpm 3'UTR-4 (AT<sub>1a</sub>R) (A) or 3'UTR-5 (AT<sub>1b</sub>R) (B) <sup>32</sup>P-labeled antisense RNA probes. After incubation, all unprotected RNA (*i.e.* any RNA not hybridized to the antisense probes) was digested with RNase T1. Shown are the 420-nt AT<sub>1a</sub>R (A, lanes 4–7), 429-nt AT<sub>1b</sub>R (B, lanes 4–7), and 250-nt β-actin RNA (A and B, lanes 4–7) radiolabeled protected fragments analyzed on 5% denaturing polyacrylamide/urea gels (note, the protected fragments are a bit smaller than the probes not treated with T1 RNase, because of the presence of 40 nt of RNA encoded by the plasmid used to generate the probes). In negative controls, AT<sub>1a</sub>R (A, lanes 2 and 3) or AT<sub>1b</sub>R (B, lanes 2 and 3) <sup>32</sup>P-labeled antisense RNA probes (35,000 cpm) were hybridized with 2.5 μg yeast RNA, followed by digestion with (A and B, lane 3) or without (A and B, lane 2) T1 RNase. Lane 1 shows the molecular weight markers (note the molecular markers in A, lane 1, have run a bit high because of gel smiling). The amounts of AT<sub>1a</sub>R- and AT<sub>1b</sub>R-protected fragments were quantitated by phosphorimaging. Shown are the ratios of AT<sub>1a</sub>R and AT<sub>1b</sub>R to β-actin in the AC (C) and pituitary (D). Values are the mean ± SEM (n = 5).

AC (Fig. 4C). In contrast, E<sub>2</sub> significantly decreased steady-state levels of AT<sub>1a</sub>R and AT<sub>1b</sub>R mRNAs in the pituitary of these same rats, by 37% (OVX, 0.33 ± 0.01; OVX + E<sub>2</sub>, 0.16 ± 0.01, *P* < 0.001 *vs.* OVX, n = 5) and 93% (OVX, 2.90 ± 0.30; OVX + E<sub>2</sub>, 0.20 ± 0.03, *P* < 0.001 *vs.* OVX, n = 5), respectively (Fig. 4D).

#### E<sub>2</sub> reduces AT<sub>1</sub>R translational efficiency in the AC

Because E<sub>2</sub> did not decrease AT<sub>1</sub>R mRNA levels in the AC, we investigated whether E<sub>2</sub> lowers AT<sub>1</sub>R density by inhibiting receptor translation. AC cytosolic extracts from OVX and E<sub>2</sub>-treated rats were layered onto sucrose gradients. After centrifugation, six equal fractions from A to F (with A comprising the heaviest polysome fraction and F, the lightest) were collected. Total RNA was extracted from each fraction and incubated with an antisense RNA probe that was complementary to an 89-nt stretch within both the AT<sub>1a</sub>R and AT<sub>1b</sub>R CRs (so both AT<sub>1a</sub>R and AT<sub>1b</sub>R mRNAs would be detected). The RPA results showed that the amount of AT<sub>1</sub>R mRNA in the most dense fraction A was 63% less in E<sub>2</sub>-treated OVX rats than in vehicle-treated OVX rats (% of total: OVX, 27 ± 2; OVX + E<sub>2</sub>, 10 ± 3, *P* < 0.005 *vs.* OVX, n = 3);

whereas in the lighter fraction C, there was 59% more AT<sub>1</sub>R mRNA in the E<sub>2</sub>-treated OVX rats than in the vehicle-treated OVX animals (% of total: OVX, 17 ± 1; OVX + E<sub>2</sub>, 27 ± 2, *P* < 0.005 *vs.* OVX, n = 3) (Fig. 5).

To confirm that the AT<sub>1</sub> mRNA fractionation in the sucrose gradient represented decreasing amounts of ribosomes bound to the AT<sub>1</sub>R mRNA from fractions A–F (rather than an artifact of RNA protein binding), AC extracts from OVX rats were run on sucrose gradients prepared in a buffer in which MgCl<sub>2</sub> was replaced by EDTA (Fig. 6) [the presence of EDTA causes mRNA and ribosomes to disassociate (28, 29)]. In these polysome disruption experiments, the AT<sub>1</sub>R mRNA was redistributed, from the majority being in fractions A–C to the majority being in the lighter fractions (D–F), indicating that the distribution of AT<sub>1</sub>R mRNA in the sucrose fractionation shown in Fig. 5 represented decreasing amounts of ribosomes bound to AT<sub>1</sub>R mRNA from heavy to light fractions.

#### E<sub>2</sub> increases cytosolic AT<sub>1a</sub>R and AT<sub>1b</sub>R 5'LS RBP activity

To determine whether RBPs bind to the AT<sub>1b</sub>R 5'LS in a similar manner as that observed in the AT<sub>1a</sub>R 5'LS (18), we

FIG. 5. Effect of E<sub>2</sub> treatment on the polysomal distribution of AC AT<sub>1</sub>R mRNA. AC cytosolic extracts from OVX rats treated with vehicle (*open bars*) or E<sub>2</sub> at 40 μg/kg·d (*filled bars*) for 8 d were homogenized and loaded onto a 10–50% sucrose gradient. After centrifugation, six equal fractions (A→F) were collected from the bottom (fraction A) to the top (fraction F) of the gradient, followed by isolation of total RNA. The amount of AT<sub>1</sub>R mRNA in each fraction was determined by RPA using the CR-4 AT<sub>1</sub>R antisense probe, which hybridized to the CR of both the AT<sub>1a</sub>R and AT<sub>1b</sub>R. Shown are the hybridization signals (*inset*) and the amount of AT<sub>1</sub>R mRNA in each fraction expressed as a percentage of the total AT<sub>1</sub>R mRNA recovered from all six fractions. \*,  $P < 0.005$ , OVX vs. OVX + E<sub>2</sub>; six animals/group constitutes one n value; n = 3.

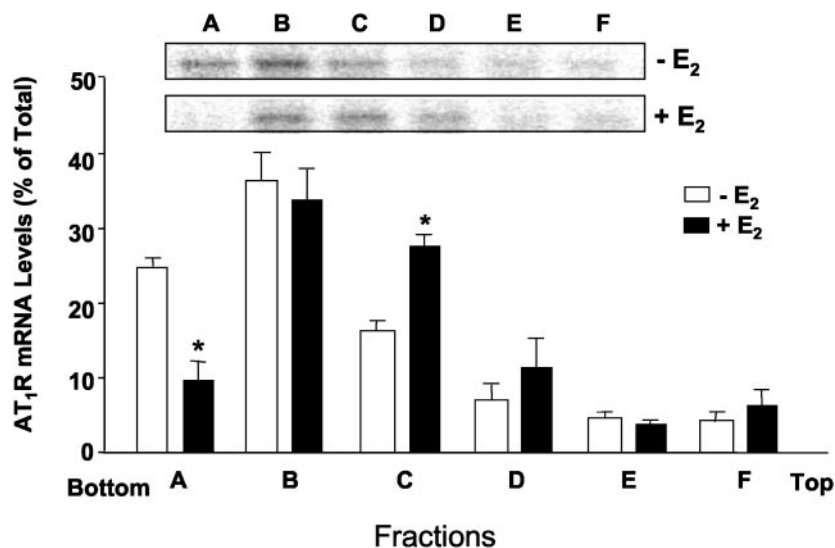
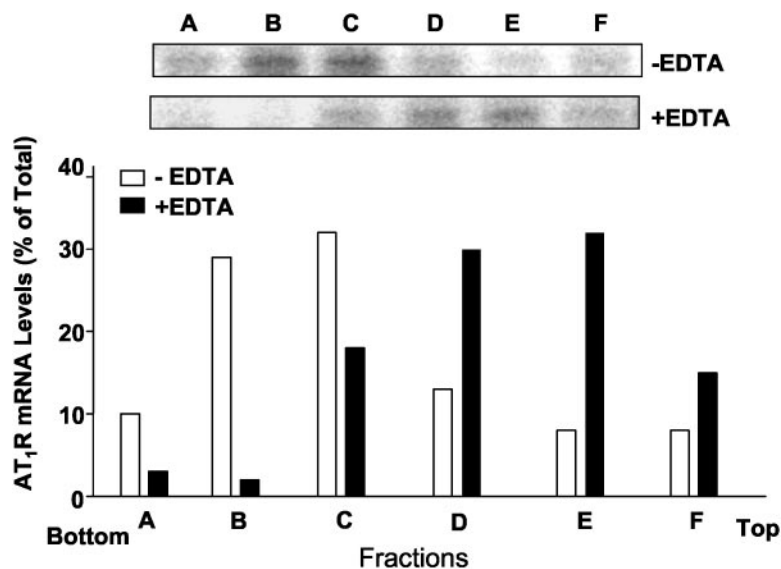


FIG. 6. Effect of EDTA on the polysome distribution of AC AT<sub>1</sub>R mRNA. AC cytosolic extracts from untreated rats were homogenized, and half the samples were loaded onto a 10–50% sucrose gradient (*open bars*), whereas the other half were loaded onto a sucrose gradient in which MgCl<sub>2</sub> was replaced with EDTA in the gradient buffer (*filled bars*). AT<sub>1</sub>R mRNA was determined from each sucrose fractionation, as in Fig. 5. Shown are the hybridization signals (*top*) and the amount of AT<sub>1</sub>R mRNA in each fraction expressed as a percentage of the total AT<sub>1</sub>R mRNA recovered from all six fractions (*bottom*).



examined the effects of E<sub>2</sub> on both AT<sub>1a</sub>R and AT<sub>1b</sub>R RBP activity in AC cytosolic fractions. We found that AC RBPs bound the 5'LS of both the AT<sub>1a</sub>R and AT<sub>1b</sub>R and that E<sub>2</sub> treatment significantly increased their RBP activity, by 148% (OVX, 1.0 ± 0.38; OVX + E<sub>2</sub>, 2.48 ± 0.37,  $P < 0.05$ , n = 3) and by 68% (OVX, 1.0 ± 0.15; OVX + E<sub>2</sub>, 1.68 ± 0.19,  $P < 0.05$ , n = 3), respectively (Fig. 7).

#### E<sub>2</sub> inhibits AT<sub>1</sub>R RBP activity to the 5'LS but not to other regions of the receptor mRNA

To determine whether E<sub>2</sub> regulates RBPs that bind to other regions of the AT<sub>1</sub>R mRNA, six different regions of the AT<sub>1</sub>R, of approximately the same size as the 5'LS, were randomly selected from the AT<sub>1</sub>R CR and 3'UTR and used as radiolabeled RNA probes to detect RBP activity. In contrast to the increased activity found in the 5'LS (OVX, 1.0 ± 0.27; OVX + E<sub>2</sub>, 2.99 ± 0.75,  $P < 0.05$ , n = 3), E<sub>2</sub> did not significantly alter RBP activity in the CR or 3'UTR (Fig. 8).

## Discussion

Most of the currently demonstrated diverse effects of estrogen are mediated by the genomic pathway involving the interaction of estrogen with a nuclear receptor protein (30). Two ER subtypes (ERα and ERβ) have thus far been cloned and characterized (31). ERα and ERβ have similar affinities for E<sub>2</sub> and bind to the same estrogen response elements (ERE), although the hormone binding domains are only 53% homologous (32). Both tissue-specific expression of ER subtypes and differences in transcriptional activation influence the effects of E<sub>2</sub> on different tissue types.

RT-PCR and RPA studies have shown that both ERα and ERβ mRNAs are present in the adrenal gland; however, protein expression was not examined in this study (33). Our results indicate that ERα and ERβ immunoreactivity is prominently expressed in the ZG of the rat AC (Fig. 1). Our findings are therefore consistent with an early radioligand binding study that demonstrated the presence of ERs in rat adrenal gland membranes; however, the radioligand used

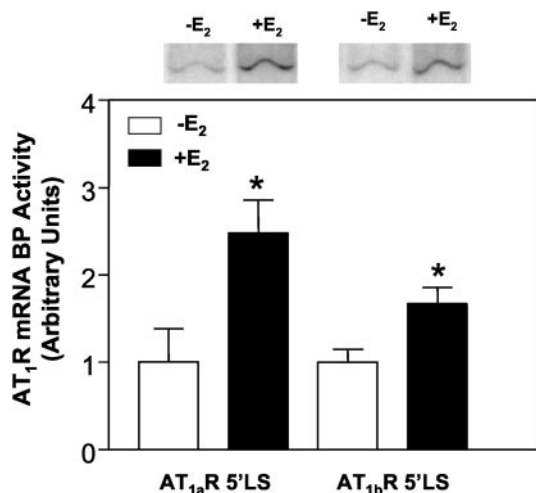


FIG. 7. Effect of E<sub>2</sub> treatment on AC AT<sub>1</sub>R 5'LS RBP activity. RNA EMSA was performed using 5'LS (AT<sub>1a</sub>R) or 5'LS (AT<sub>1b</sub>R) <sup>32</sup>P-labeled RNA probes (100,000 cpm) and AC cytosolic extracts (40 μg) prepared from OVX rats treated with vehicle (open bars) or E<sub>2</sub> at 40 μg/kg (filled bars) for 8 d. Shown are EMSA autoradiograms (top) quantitated by phosphorimaging (in arbitrary units) and expressed as a ratio of radioactivity from the E<sub>2</sub>-treated OVX rats normalized to the average radioactivity from the OVX group (-E<sub>2</sub>). \*, *P* < 0.05, OVX vs. OVX + E<sub>2</sub>; two animals/group constitutes one n value; n = 3.

could not differentiate between ERα and ERβ subtypes (34). Our findings also support a previous immunohistochemistry study in rhesus monkey adrenal glands that showed ER immunoreactivity using an antibody that did not distinguish between ER subtypes (35). Our demonstration that both ER subtype antigens are expressed suggests that both the ERα and ERβ mRNAs found in the adrenal gland (33) are translated into protein. Furthermore, our finding that ERα and ERβ immunoreactivity is present in the ZG suggests that either of these ER subtypes could play a role in E<sub>2</sub> modulation of AT<sub>1</sub>R density and Ang II-induced aldosterone release from the ZG, whereas any estrogen action in the adrenal medulla is likely to be ERα-mediated, because ERβ was undetectable in this region.

The apparent increase in immunoreactive nuclear staining for both ER subtypes in the E<sub>2</sub>-treated OVX rats suggests that E<sub>2</sub> may up-regulate the expression of its own receptors in the AC (Fig. 1). This observed increase in immunoreactive nuclear staining for ERα, after E<sub>2</sub> treatment, is consistent with previous reports in human myometrium and mouse testis showing that estrogen can up-regulate ERα expression (36, 37). However (unlike our finding that E<sub>2</sub> treatment also increased ERβ expression in the ZG), in the myometrium and testis, estrogen treatment decreased ERβ (36, 37). Of interest is the observation that the intensity of ERα staining was more prominent in the nucleus than in the cytoplasm after E<sub>2</sub> treatment, suggesting that E<sub>2</sub> induces the relocation or retention of ERs into the cell nuclei. Changes in the cytoplasmic pattern of ERα immunolocalization were also observed in a cultured rat pituitary tumor cell line (38).

Recent studies showed that ERβ mRNA expression was markedly increased after intravascular balloon injury (39), and a recent report (40) demonstrated that ERβ-deficient mice have abnormal vascular function and develop hyper-

tension with increasing age. These provocative new findings suggest that ERβ may play a role in the vascular protective effects of E<sub>2</sub>.

We previously showed that 1 wk of E<sub>2</sub> treatment in OVX rats significantly reduced AT<sub>1</sub>R expression in adrenal gland membranes (18, 41). In this study, we found significant effects of E<sub>2</sub> on AT<sub>1</sub>R density after only 2 d of E<sub>2</sub> treatment in OVX rats; however, maximal effects were not observed until after 1 wk of treatment (Fig. 2). This relatively long time course suggests that AT<sub>1</sub>R expression is altered by mechanisms involving gene expression, such as transcription, translation, and protein turnover, rather than by rapid regulation of signal transduction pathways.

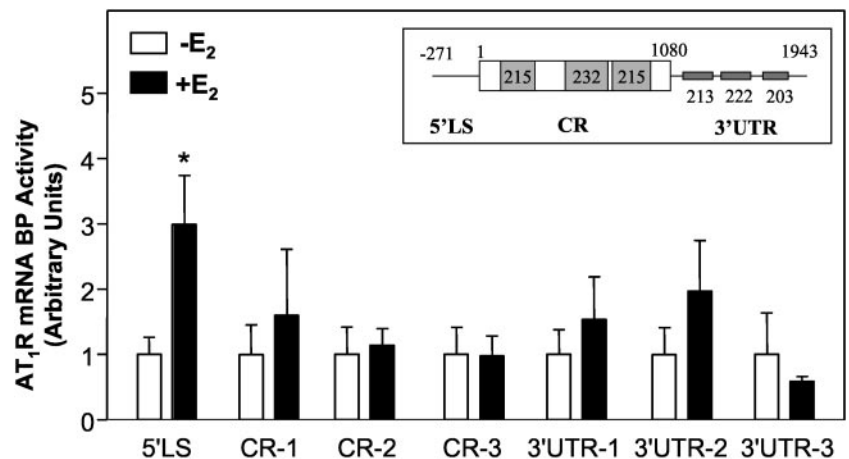
At doses of E<sub>2</sub> that reflect peak physiological levels in female rats (27), AT<sub>1</sub>R expression was inhibited by approximately 30% in the whole adrenal gland and by 46% in the AC. Under these conditions, we found that E<sub>2</sub> decreased aldosterone release by 43% in rats infused chronically with Ang II (Fig. 3). These new findings support our previous studies demonstrating that E<sub>2</sub> treatment of OVX rats significantly reduced acute Ang II-induced aldosterone release (41). The fact that estrogen also reduced plasma aldosterone levels after chronic Ang II infusions further supports the concept that attenuation of aldosterone responses contributes to the cardioprotective effects associated with estrogen. Thus, it will be very interesting to determine whether ERβ-deficient mice have abnormal Ang II-induced aldosterone responses that might contribute to their vascular function defects and the hypertension that develops in these animals with age (40).

Two highly homologous subtypes of the AT<sub>1</sub>R (95% at the amino acid level), termed AT<sub>1a</sub>R and AT<sub>1b</sub>R, have been cloned in rodents (24). These receptors are pharmacologically and functionally highly similar; and, thus far, immunohistochemistry and radioligand binding techniques have not been able to distinguish between them; however, their mRNAs are distinguishable because of lack of homology in the 5'LS and 3'UTRs. Whereas the AT<sub>1a</sub>R is widely distributed, the AT<sub>1b</sub>R is predominantly localized to the pituitary and adrenal gland; AT<sub>1b</sub>Rs comprise 52% of the total AT<sub>1</sub>R mRNA population (AT<sub>1a</sub>R + AT<sub>1b</sub>R) in the adrenal (42) and represent the majority of AT<sub>1</sub>R mRNA in the anterior pituitary (43).

E<sub>2</sub> markedly decreased AT<sub>1a</sub>R and AT<sub>1b</sub>R mRNA in the rat pituitary, suggesting that E<sub>2</sub> decreases AT<sub>1</sub>R densities in that tissue by inhibiting receptor transcription. Both the ERα and ERβ receptors modulate gene transcription through ERE and AP-1 enhancer elements present in estrogen-regulated genes; and both receptor subtypes were shown to be present in the pituitary, by immunohistochemistry and Western blotting (44). Thus, estrogen could regulate AT<sub>1a</sub>R gene transcription in the pituitary at these ERE and AP-1 regulatory elements, because they have been identified in the 5' flanking region of the AT<sub>1a</sub>R gene (45, 46). Because the 5' flanking region of the rat AT<sub>1b</sub>R gene is yet to be characterized, it is unknown whether these same elements also exist in the AT<sub>1b</sub>R. Though both ERs activate gene transcription through ERE, ERα and ERβ function in opposition through AP-1 sites. ERβ actually suppresses the function of ERα through AP-1-mediated gene transactivation (47). The finding that estrogen coordinately



FIG. 8. Effect of E<sub>2</sub> treatment on AC AT<sub>1</sub>R 5'LS, CR, and 3'UTR RBP activities. RNA EMSA was performed using 5'LS (AT<sub>1a</sub>R), CR-1, CR-2, CR-3, 3'UTR-1, 3'UTR-2, or 3'UTR-3 <sup>32</sup>P-labeled RNA probes (100,000 cpm) and AC cytosolic extracts (40 μg) prepared from OVX rats treated with vehicle (open bars) or E<sub>2</sub> at 40 μg/kg (filled bars) for 8 d. Shown are EMSA autoradiograms quantitated by phosphorimaging (in arbitrary units) and expressed as a ratio of radioactivity from the E<sub>2</sub>-treated OVX rats normalized to the average radioactivity from the OVX group (–E<sub>2</sub>). \*, P < 0.05, OVX vs. OVX + E<sub>2</sub>; two animals/group constitutes one n value; n = 3. Inset, Location of the RNA probes within the AT<sub>1a</sub>R cDNA.



decreases the mRNA for both the AT<sub>1a</sub>R and AT<sub>1b</sub>R subtypes in the pituitary suggests that differential estrogen regulation through AP-1 sites is not occurring.

The surprising finding that E<sub>2</sub> did not decrease expression of either AT<sub>1a</sub>R or AT<sub>1b</sub>R mRNA in the AC (Fig. 4) suggests that E<sub>2</sub> does not down-regulate AT<sub>1</sub>R number primarily by inhibiting AT<sub>1</sub>R transcription in this tissue. Though the possibility remains that E<sub>2</sub> decreases adrenal AT<sub>1</sub>R transcription at the same time as stabilizing AT<sub>1</sub>R mRNA, resulting in equivalent steady-state levels of adrenal AT<sub>1</sub>R mRNA, this scenario is unlikely, because inhibition of transcription is commonly accompanied by reduced mRNA expression.

One explanation for these tissue-specific differences is that the function of the AT<sub>1</sub>R is different in these tissues. In the adrenal, the AT<sub>1</sub>R mediates aldosterone secretion in response to rapid changes in Ang II levels. Under conditions of changing Ang II levels, the body must respond quickly to preserve fluid and electrolyte homeostasis to maintain stable blood pressure and cardiac output. Thus, having cellular stores of AT<sub>1</sub>R mRNA that are ready to be translated would represent a more rapid method for changing AT<sub>1</sub>R protein expression in response to acute stimuli than having to wait for the cell to first transcribe the DNA before translating the mRNA into AT<sub>1</sub>R protein. In contrast, in the pituitary, AT<sub>1</sub>Rs are involved in more chronic responses, such as mediation of prolactin and TSH secretion. Thus, transcriptional regulation of AT<sub>1</sub>Rs in the pituitary may represent an appropriate mechanism for controlling AT<sub>1</sub>R expression there.

The lack of AT<sub>1</sub>R mRNA regulation by E<sub>2</sub> in the AC suggested that E<sub>2</sub> mediates its inhibition of AT<sub>1</sub>R number in the ZG by posttranscriptional mechanisms. Therefore, we developed a polysome distribution assay to study the effects of E<sub>2</sub> on AT<sub>1</sub>R translational efficiency *in vivo*. During translation initiation, 40S and 60S ribosome subunits assemble on the mRNA to form an 80S monosome or ribosome. The ribosome moves along the mRNA and then dissociates into subunits upon termination. Sucrose density gradients can separate polysomes according to their size, which is determined by the number of ribosomes bound to the mRNA. The mRNAs with the most polysomes bound will be the heaviest and, thus, found in the bottom fraction of the sucrose gradient, whereas the top fractions generally consist of monosomes,

ribosomal subunits, and material sedimenting more slowly than the ribosomal subunits.

The fact that E<sub>2</sub> treatment of OVX rats shifted the AT<sub>1</sub>R mRNA profile from the denser to lighter polysome fractions (Fig. 5) suggests that E<sub>2</sub> reduces the efficiency of AT<sub>1</sub>R translation initiation, because the extent of ribosome loading on a mRNA depends primarily on the rates of translation initiation. Thus, mRNAs found in the heaviest sucrose fractions are translated more efficiently than those mRNAs located in the lighter sucrose fractions (25, 26), and a block in translation would result in the accumulation of small-sized polysomes and monosomes (26). However, the caveat remains that if elongation or termination were inhibited under these conditions, the rate of ribosome movement would slow down, as would the rate of protein synthesis; this scenario, however, is unlikely, because inhibition of elongation and termination are rarely rate limiting. Taken together, the results of the RPA and polysomal distribution analysis strongly suggest that E<sub>2</sub> modulation of AT<sub>1</sub>R density in the AC is mediated at the posttranscriptional level by inhibiting receptor mRNA translation.

Although most reported studies of estrogen action have focused on control of gene expression at the level of transcription, estrogen has also been shown to act posttranscriptionally at the level of mRNA stability and translation. Estrogen activates a polysome-associated endonuclease and thereby destabilizes serum protein mRNAs in estrogen-treated frogs (48). Estrogen has also been shown to shift the distribution of ornithine δ-aminotransferase (OAT) mRNAs in neuroblastoma cells to denser fractions on a polysome gradient, suggesting that estrogen acts to increase OAT translation initiation (49). Our results are particularly interesting because, to our knowledge, this is the first study suggesting that E<sub>2</sub> can also modulate G protein-coupled receptor translation.

In genes that are regulated posttranscriptionally, RNA *trans*-acting factors are found to play a key role in gene expression by altering translational efficiency and/or mRNA stability (50, 51). We previously showed that cytosolic proteins in the adrenal bind to the 5'LS of the AT<sub>1a</sub>R and that the activity of these RBPs is modulated by E<sub>2</sub> in whole adrenal cytosolic extracts (18); however, we did not determine

whether cytosolic RBPs also bind to the AT<sub>1b</sub>R or whether these cytosolic proteins are located in the ZG, the tissue responsible for Ang II-induced aldosterone release. The observation that 5'LS AT<sub>1</sub>R RBP activities are up-regulated under conditions in which the polysome distribution analysis indicates that E<sub>2</sub> is inhibiting AT<sub>1</sub>R translation efficiency (Fig. 5), suggests that these 5'LS RBPs play a role in the mechanism by which E<sub>2</sub> reduces Ang II-induced aldosterone secretion from the ZG.

Numerous studies have shown that RBPs can recognize sequences in the CR and 3'UTR of mRNAs. A 50-kDa protein was shown to bind the CR of the LH/human chorionic gonadotropin receptor mRNA and was associated with destabilization of the receptor mRNA (52). In addition, FOS and MYC mRNAs contain a 180–320 purine-rich nucleotide segment in their CRs for RNA protein binding (53). Proteins were also found to bind with high specificity to the stem-loop structure located in the 3'UTR of the histone mRNA and to affect the histone mRNA transport, translation, and half-life (54). RBPs has been reported to bind to the 3'UTR of AT<sub>1</sub>R and to regulate mRNA stability. In rat vascular smooth muscle cells, RBPs specifically bound to the distal 350 bases of the AT<sub>1a</sub>R mRNA and are likely involved in the Ang II-induced AT<sub>1a</sub>R mRNA destabilization (55). In Chinese hamster ovary cells, a major cellular protein of 55 kDa was identified and found to specifically interact with the 3'UTR of the AT<sub>1a</sub>R, to control mRNA stability (56). In human vascular smooth muscle cells, the RNA binding protein, AUF1, has been shown to bind the AU-rich regions of the 3'UTR of AT<sub>1</sub>Rs and to regulate receptor expression by altering mRNA levels (57).

According to the so-called scanning theory of protein translation (58), the formation of RBP activity in the 5'LS of receptor mRNAs could cause steric hindrance and thereby block the scanning of small ribosomal subunits toward the downstream open reading frame, so that translation efficiency is reduced. Posttranscriptional regulation by 5'LS RBPs has been reported to be an efficient way to regulate ferritin, erythroid 5'-aminoevulinate synthase, and folate receptor- $\alpha$  expression (59, 60). Thus, the observation that E<sub>2</sub> does not regulate RBP activity in the CR or 3'UTR suggests that the mechanisms by which E<sub>2</sub> reduces AT<sub>1</sub>R expression in the AC primarily involve 5'LS RBPs.

In summary, our results suggest that, in the rat AC, E<sub>2</sub> reduces AT<sub>1</sub>Rs and Ang II-induced aldosterone release by a posttranscriptional mechanism in which AT<sub>1</sub>R translational efficiency is inhibited. Our results showing that E<sub>2</sub> regulates RBP activity in the 5'LS, but not in the CR or 3'UTR of the AT<sub>1</sub>R mRNA, further supports our hypothesis that E<sub>2</sub> reduces AT<sub>1</sub>R translation in the AC by inhibiting ribosomal scanning attributable to increased steric hindrance from 5'LS RBPs. In addition to furthering our understanding of the molecular mechanisms underlying estrogen modulation of AT<sub>1</sub>Rs and Ang II-induced aldosterone release, our data raise the possibility that dysregulation of this E<sub>2</sub>-mediated posttranscriptional mechanism contributes to the increased incidence of cardiovascular disease observed after menopause, deriving from a loss in E<sub>2</sub>-mediated attenuation of Ang II-induced aldosterone responses.

## Acknowledgments

This research was supported by NIH Grants HL-57502 (to K.S.) and AG-19291 (to K.S.).

Received January 6, 2003. Accepted March 26, 2003.

Address all correspondence and requests for reprints to: Kathryn Sandberg, Ph.D., Building D, Room 394, Georgetown University Medical Center, 4000 Reservoir Road, NW, Washington, D.C. 20007. E-mail: sandberg@georgetown.edu.

## References

- Castelli WP 1988 Cardiovascular disease in women. *Am J Obstet Gynecol* 158:1553–1560, 1566–1567
- Rossouw JE, Anderson GL, Prentice RL, LaCroix AZ, Kooperberg C, Stefanick ML, Jackson RD, Beresford SA, Howard BV, Johnson KC, Kotchen JM, Ockene J 2002 Risks and benefits of estrogen plus progestin in healthy postmenopausal women: principal results from the Women's Health Initiative randomized controlled trial. *JAMA* 288:321–333
- Sandberg K 2002 HRT and SERMs: the good, the bad . . . and the lovely? *Trends Endocrinol Metab* 13:317
- Nasr A, Breckwoldt M 1998 Estrogen replacement therapy and cardiovascular protection: lipid mechanisms are the tip of an iceberg. *Gynecol Endocrinol* 12:43–59
- Schunkert H, Danser AH, Hense HW, Derckx FH, Kurzinger S, Riegger GA 1997 Effects of estrogen replacement therapy on the renin-angiotensin system in postmenopausal women. *Circulation* 95:39–45
- Harvey PJ, Wing LM, Savage J, Molloy D 1999 The effects of different types and doses of oestrogen replacement therapy on clinic and ambulatory blood pressure and the renin-angiotensin system in normotensive postmenopausal women. *J Hypertens* 17:405–411
- Nabulsi AA, Folsom AR, White A, Patsch W, Heiss G, Wu KK, Szklo M 1993 Association of hormone-replacement therapy with various cardiovascular risk factors in postmenopausal women. The atherosclerosis risk in communities study investigators. *N Engl J Med* 328:1069–1075
- Stampfer MJ, Colditz GA, Willett WC, Manson JE, Rosner B, Speizer FE, Hennekens CH 1991 Postmenopausal estrogen therapy and cardiovascular disease. Ten-year follow-up from the nurses' health study. *N Engl J Med* 325:756–762
- Barrett-Connor E, Bush TL 1991 Estrogen and coronary heart disease in women. *JAMA* 265:1861–1867
- Gerhard M, Ganz P 1995 How do we explain the clinical benefits of estrogen? From bedside to bench. *Circulation* 92:5–8
- Mosca L, Manson JE, Sutherland SE, Langer RD, Manolio T, Barrett-Connor E 1997 Cardiovascular disease in women: a statement for healthcare professionals from the American Heart Association. Writing Group. *Circulation* 96:2468–2482
- Corvol P, Jeunemaitre X, Charru A, Kotelevtsev Y, Soubrier F 1995 Role of the renin-angiotensin system in blood pressure regulation and in human hypertension: new insights from molecular genetics. *Recent Prog Horm Res* 50:287–308
- Klett C, Ganten D, Hellmann W, Kaling M, Ryffel GU, Weimar-Ehl T, Hackenthal E 1992 Regulation of angiotensinogen synthesis and secretion by steroid hormones. *Endocrinology* 130:3660–3668
- Brosnihan KB, Weddle D, Anthony MS, Heise C, Li P, Ferrario CM 1997 Effects of chronic hormone replacement on the renin-angiotensin system in cynomolgus monkeys. *J Hypertens* 15:719–726
- Gallagher PE, Li P, Lenhart JR, Chappell MC, Brosnihan KB 1999 Estrogen regulation of angiotensin-converting enzyme mRNA. *Hypertension* 33:323–328
- Seltzer A, Tsutsumi K, Shigematsu K, Saavedra JM 1993 Reproductive hormones modulate angiotensin II AT<sub>1</sub> receptors in the dorsomedial arcuate nucleus of the female rat. *Endocrinology* 133:939–941
- Nickenig G, Baumer AT, Grohe C, Kahlert S, Strehlow K, Rosenkranz S, Stablain A, Beckers F, Smits JF, Daemen MJ, Vetter H, Bohm M 1998 Estrogen modulates AT<sub>1</sub> receptor gene expression *in vitro* and *in vivo*. *Circulation* 97:2197–2201
- Krishnamurthi K, Verbalis JG, Zheng W, Wu Z, Clerch LB, Sandberg K 1999 Estrogen regulates angiotensin AT<sub>1</sub> receptor expression via cytosolic proteins that bind to the 5' leader sequence of the receptor mRNA. *Endocrinology* 140:5431–5434
- Rosenfeld CR, Jackson GM 1984 Estrogen-induced refractoriness to the pressor effects of infused angiotensin II. *Am J Obstet Gynecol* 148:429–435
- Roesch DM, Tian Y, Zheng W, Shi M, Verbalis JG, Sandberg K 2000 Estradiol attenuates angiotensin-induced aldosterone secretion in ovariectomized rats. *Endocrinology* 141:4629–4636
- Rahmouni K, Barthelmebs M, Grima M, Imbs JL, Wybren De J 1999 Brain mineralocorticoid receptor control of blood pressure and kidney function in normotensive rats. *Hypertension* 33:1201–1206
- Brownie AC 1995 The adrenal cortex in hypertension: DOCA/salt hyperten-

- sion and beyond. In: Laragh JH, ed. Hypertension: pathophysiology, diagnosis, and management. Philadelphia: Lippincott Williams & Wilkins; 2127
23. Pitt B, Zannad F, Remme WJ, Cody R, Castaigne A, Perez A, Palensky J, Wittes J 1999 The effect of spironolactone on morbidity and mortality in patients with severe heart failure. Randomized Aldactone Evaluation Study investigators [see comments]. *N Engl J Med* 341:709–717
  24. Sandberg K, Ji H, Clark AJ, Shapira H, Catt K 1992 Cloning and expression of a novel rat angiotensin II receptor subtype. *J Biol Chem* 267:9455–9458
  25. Saggiocco FA, Moore PA, Brown AJP 1996 Polysome analysis. *Methods Mol Biol* 53:297–311
  26. Davies E, Abe S 1995 Methods for isolation and analysis of polyribosomes. *Methods Cell Biol* 50:209–222
  27. Henderson SR, Baker C, Fink G 1977 Oestradiol-17 $\beta$  and pituitary responsiveness to luteinizing hormone releasing factor in the rat: a study using rectangular pulses of oestradiol-17 $\beta$  monitored by non-chromatographic radioimmunoassay. *J. Endocrinol* 73:441–453
  28. Hagen HG, Giorgini F, Fajardo MA, Braun RE 2000 A sequence-specific RNA binding complex expressed in murine germ cells contains MSY2 and MSY4. *Dev Biol* 221:87–100
  29. Tena-Sempere M, Rannikko A, Kero J, Zhang FP, Huhtaniemi IT 1997 Molecular mechanisms of reappearance of luteinizing hormone receptor expression and function in rat testis after selective Leydig cell destruction by ethylene dimethane sulfonate. *Endocrinology* 138:3340–3348
  30. Parker MG 1995 Structure and function of estrogen receptors. *Vitam Horm* 51:267–287
  31. Brandenberger AW, Tee MK, Lee JY, Chao V, Jaffe RB 1997 Tissue distribution of estrogen receptors  $\alpha$  (ER- $\alpha$ ) and  $\beta$  (ER- $\beta$ ) mRNA in the midgestational human fetus. *J Clin Endocrinol Metab* 82:3509–3512
  32. Curtis SH, Korach KS 2000 Steroid receptor knockout models: phenotypes and responses illustrate interactions between receptor signaling pathways *in vivo*. *Adv Pharmacol* 47:357–380
  33. Couse JF, Korach KS 1999 Estrogen receptor null mice: what have we learned and where will they lead us? [published erratum appears in *Endocr Rev* 20:459]. *Endocr Rev* 20:358–417
  34. Hagenfeldt Y, Eriksson HA 1988 The estrogen receptor in the rat kidney. Ontogeny, properties and effects of gonadectomy on its concentration. *J Steroid Biochem* 31:49–56
  35. Hirst JJ, West NB, Brenner RM, Novy MJ 1992 Steroid hormone receptors in the adrenal glands of fetal and adult rhesus monkeys. *J Clin Endocrinol Metab* 75:308–314
  36. Takao T, Nanamiya W, Nazarloo HP, Matsumoto R, Asaba K, Hashimoto K 2003 Exposure to the environmental estrogen bisphenol A differentially modulated estrogen receptor- $\alpha$  and - $\beta$  immunoreactivity and mRNA in male mouse testis. *Life Sci* 72:1159–1169
  37. Sakaguchi H, Fujimoto J, Aoki I, Tamaya T 2002 Expression of estrogen receptor  $\alpha$  and  $\beta$  in myometrium of premenopausal and postmenopausal women. *Steroids* 68:11–19
  38. Campbell CH, Bulayeva N, Brown DB, Gametchu B, Watson CS 2002 Regulation of the membrane estrogen receptor- $\alpha$ : role of cell density, serum, cell passage number, and estradiol. *FASEB J* 16:1917–1927
  39. Lindner V, Kim SK, Karas RH, Kuiper GG, Gustafsson JA, Mendelsohn ME 1998 Increased expression of estrogen receptor- $\beta$  mRNA in male blood vessels after vascular injury. *Circ Res* 83:224–229
  40. Zhu Y, Bian Z, Lu P, Karas RH, Bao L, Cox D, Hodgins J, Shaul PW, Thoren P, Smithies O, Gustafsson JA, Mendelsohn ME 2002 Abnormal vascular function and hypertension in mice deficient in estrogen receptor  $\beta$ . *Science* 295:505–508
  41. Roesch D, Zheng W, Tian Y, Verbalis JG, Sandberg K 1999 Estrogen decreases angiotensin-induced aldosterone production and adrenal AT<sub>1</sub> receptor expression in ovariectomized rats. *J Am Soc Nephrol* 10:461a
  42. Llorens-Cortes C, Greenberg B, Huang H, Corvol P 1994 Tissue expression and regulation of type 1 angiotensin II receptor subtypes by quantitative reverse transcriptase-polymerase chain reaction analysis. *Hypertension* 24:538–548
  43. Gasc JM, Shanmugam S, Sibony M, Corvol P 1994 Tissue-specific expression of type 1 angiotensin II receptor subtypes. An *in situ* hybridization study. *Hypertension* 24:531–537
  44. Nishihara E, Nagayama Y, Inoue S, Hiroi H, Muramatsu M, Yamashita S, Koji T 2000 Ontogenetic changes in the expression of estrogen receptor  $\alpha$  and  $\beta$  in rat pituitary gland detected by immunohistochemistry. *Endocrinology* 141:615–620
  45. Takeuchi K, Alexander RW, Nakamura Y, Tsujino T, Murphy TJ 1993 Molecular structure and transcriptional function of the rat vascular AT<sub>1a</sub> angiotensin receptor gene. *Circ Res* 73:612–621
  46. Langford K, Frenzel K, Martin BM, Bernstein KE 1992 The genomic organization of the rat AT<sub>1</sub> angiotensin receptor. *Biochem Biophys Res Commun* 183:1025–1032
  47. Maruyama S, Fujimoto N, Asano K, Ito A 2001 Suppression by estrogen receptor  $\beta$  of AP-1 mediated transactivation through estrogen receptor  $\alpha$ . *J Steroid Biochem Mol Biol* 78:177–184
  48. Hanson MN, Schoenberg DR 2001 Identification of *in vivo* mRNA decay intermediates corresponding to sites of *in vitro* cleavage by polysomal ribonuclease 1. *J Biol Chem* 276:12331–12337
  49. Fagan RJ, Rozen R 1993 Translational control of ornithine-delta-aminotransferase (OAT) by estrogen. *Mol Cell Endocrinol* 90:171–177
  50. McCarthy JE, Kollmus H 1995 Cytoplasmic mRNA-protein interactions in eukaryotic gene expression. *Trends Biochem Sci* 20:191–197
  51. Burd CG, Dreyfuss G 1994 Conserved structures and diversity of functions of RNA-binding proteins. *Science* 265:615–621
  52. Kash JC, Menon KM 1998 Identification of a hormonally regulated luteinizing hormone/human chorionic gonadotropin receptor mRNA binding protein. Increased mRNA binding during receptor down-regulation. *J Biol Chem* 273:10658–10664
  53. Prokopcak RD, Herrick DJ, Ross J 1994 Purification and properties of a protein that binds to the C-terminal coding region of human c-myc mRNA. *J Biol Chem* 269:9261–9269
  54. Pandey NB, Williams AS, Sun JH, Brown VD, Bond U, Marzluff WF 1994 Point mutations in the stem-loop at the 3' end of mouse histone mRNA reduce expression by reducing the efficiency of 3' end formation. *Mol Cell Biol* 14:1709–1720
  55. Nickenig G, Murphy TJ 1996 Enhanced angiotensin receptor type 1 mRNA degradation and induction of polyribosomal mRNA binding proteins by angiotensin II in vascular smooth muscle cells. *Mol Pharmacol* 50:743–751
  56. Thekkumkara TJ, Thomas WG, Motel TJ, Baker KM 1998 Functional role for the angiotensin II receptor (AT<sub>1A</sub>) 3'-untranslated region in determining cellular responses to agonist: evidence for recognition by RNA binding proteins. *Biochem J* 329:255–264
  57. Pende A, Giacche M, Castigliola L, Contini L, Passerone G, Patrone M, Port JD, Lotti G 1999 Characterization of the binding of the RNA-binding protein AUF1 to the human AT(1) receptor mRNA. *Biochem Biophys Res Commun* 266:609–614
  58. Hershey JW 1991 Translational control in mammalian cells. *Annu Rev Biochem* 60:717–755
  59. Klausner RD, Rouault TA 1993 A double life: cytosolic aconitase as a regulatory 5'LS BP. *Mol Biol Cell* 4:1–5
  60. Gray NK, Hentze MW 1994 Iron regulatory protein prevents binding of the 43S translation pre-initiation complex to ferritin and eALAS mRNAs. *EMBO J* 13:3882–3891